VERSITA

GEOCHRONOMETRIA 40(4) 2013: 304-310
DOI 10.2478/s13386-013-0124-7

Available online at
www.springerlink.com

RAPID DENUDATION OF HIGHER HIMALAYA DURING LATE PLIESTOCENCE, EVIDENCE FROM OSL THERMOCHRONOLOLGY

SHARMISTHA DE SARKAR[1], GEORGE MATHEW[1], KANCHAN PANDE[1], NAVEEN CHAUHAN[2] and ASHOK K. SINGHVI[2]

[1]*Department of Earth Sciences, Indian Institute of Technology Bombay, Powai, Mumbai, India – 400076*
[2]*2Geosciences Division, Physical Research Laboratory, Navrangpura, Ahmedabad, India – 380009*

Received 31 January 2013 Accepted 4 July 2013

Abstract: Optically Stimulated Luminescence (OSL) of quartz, with closure temperatures of 30-35°C in conjunction with Apatite Fission Track (AFT; closure temp. ~120°C) and ^{40}Ar-^{39}Ar (biotite closure temperature ~350°C), were used to obtain cooling ages from Higher Himalayan crystalline rocks of Western Arunachal Himalaya (WAH). Cooling age data based on OSL, AFT and Ar-Ar thermochronology provide inference on the exhumation – erosion history for three different time intervals over million to thousand year scale.

Steady-state exhumation of ~0.5 mm/yr was observed during Miocene (>7.2 Ma) till Early Pleistocene (1.8 Ma). Onset of Pleistocene glacial/interglacial conditions from ~1.8 Ma formed glaciated valleys and rapid erosion with rivers incising deep valleys along their course. Erosion enables mid-crustal partial melts to move beneath the weak zone in the valley and causes an erosion-induced tectonic uplift. This resulted in a rapid increase in exhumation rate. The OSL thermochronology results suggest increased erosion over ~21 ka period from Late Pleistocene (2.5 mm/yr) to Early Holocene (5.5 mm/yr) and these are to be contrasted with pre 1.8 Ma erosion rate of 0.5 mm/yr. Enhanced erosion in the later stage coincides with the periods of de-glaciation during Marine Isotope Stages (MIS) 1 and 2. The results of the present study suggest that in the present setting OSL thermochronology informed on the short-term climatic effect on landscape evolution and techniques like the AFT and ^{40}Ar-^{39}Ar provided longer-term exhumation histories.

Keywords: OSL thermochronology, apatite fission track, ^{40}Ar-^{39}Ar thermochronology, Eastern Himalaya, erosion, denudation.

1. INTRODUCTION

Himalaya is a classic example of compressional orogenic system created by the cenozoic collision between the Indian and Asian Plates. Structure and high relief of Himalaya make it an ideal laboratory to study diverse geological process and factors related to mountain building. However, to understand these processes and the factors that control topographic relief and landscape evolution, it is necessary to quantify the relative efficacy of the glacial, fluvial and hill slope processes (Burbank, 2002; Herman and Braun, 2006; Whipple, 2009 and references therein). Decoupling the contributions of tectonics and climate on mountain building still remains intricate as both processes act on different time scales. Tectonics control long-term topography evolution processes while climate affects topographic reliefs over relatively shorter time span. In order to measure spatial and tem-

Corresponding author: G. Mathew
e-mail:gmathew@iitb.ac.in

ISSN 1897-1695 (online), 1733-8387 (print)

poral scale erosion rates due to glacial and fluvial actions, Optically Stimulated Luminescence (OSL) provides a method over the time scale <50-100ka.

Thermochronology is the study of the time-temperature history of rocks during their cooling and provides estimates of the time since the rocks passed through a given closure temperature (Reiners *et al.*, 2005). The thermal field of the uppermost crust is sensitive to topography and therefore, chronometric systems that have low closure temperature can inform on the history of the evolution and the timing of associated climate/tectonic processes (Ehlers, 2005). Amongst the Low Temperature Thermochronology techniques, the Fission Track (FT) thermochronometry using Zircon-Apatite (ZFT-AFT), U-Th/He dating of zircon – apatite, and $^{4}He/^{3}He$ has been used recently to understand glacial activity and topographic evolution (Shuster *et al.*, 2005; Valla *et al.*, 2011). These techniques have closure temperatures in the range of ~60-250°C and hence do not provide information on the most recent Earth history. A novel thermochronological method, based on optically stimulated luminescence (OSL) dating with a closure temperature of about 25-40°C, was recently introduced by Herman *et al.* (2010). In an analogous application the present study used OSL of quartz grains from rocks, from a region of near vertical relief in the Greater Himalaya of Western Arunachal Pradesh (**Fig. 1**). OSL thermochronology study was carried out on samples on which ^{40}Ar-^{39}Ar and Apatite Fission Track (AFT) thermochronometry data were available. The study enabled to examine the denudation rates during Late Pleistocene.

2. GEOLOGICAL SETTING AND SAMPLING

Successive underthrusting of the Indian crust beneath the Eurasian plate created orogenic wedges extending towards south of the suture zone (Gansser, 1983; Hodges, 2000; Yin *et al.*, 2006). The South Tibetan Detachment System (STDS) separates Tethyan Himalayan rocks from underlying Greater Himalayan Sequence (GHS). The Main Central Thrust (MCT) placed GHS over Lesser Himalayan Sequence (LHS). The Main Boundary Thrust (MBT) thrusts LHS over late Tertiary molasse deposits. Himalayan Frontal Thrust (HFT) is the youngest southern most active fault and this placed Late Tertiary-Quaternary deposits over present day alluvium of Indo-Gangetic Plains (**Fig. 1**).

Thermochronological studies using OSL were carried out on samples collected at a regular intervals with their elevation ranging from 3718 m close to mountain top to 1726 m in a valley along a near vertical transect from the north to south of Tawang (**Fig. 2**). Elevations of samples were recorded using an altimeter with a measurement uncertainty of ±10 m. The samples are high grade metamorphic rocks dominantly garnet – sillimanite bearing paragneiss and migmatitic gneiss. Exhumation or denudation rate of rocks from such steep slopes can be computed

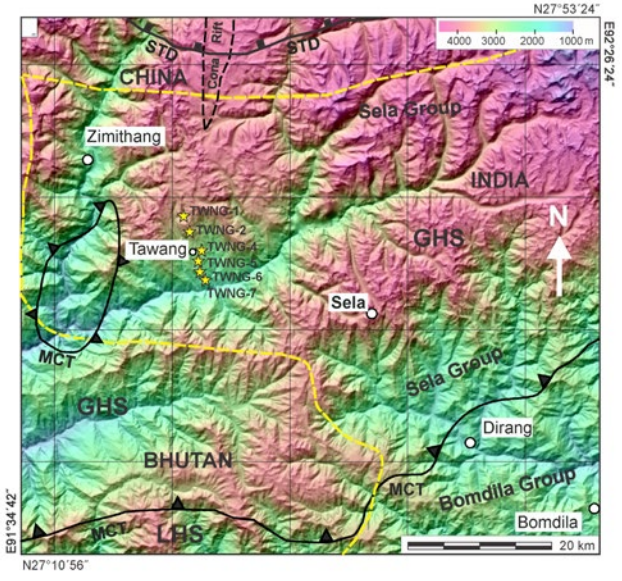

Fig. 2. *DEM image of the study area showing regional structure and topographic relief. The star symbol shows the sample locations for thermochronometry analysis from the Greater Himalayan rocks. The samples were collected along a near vertical profile.*

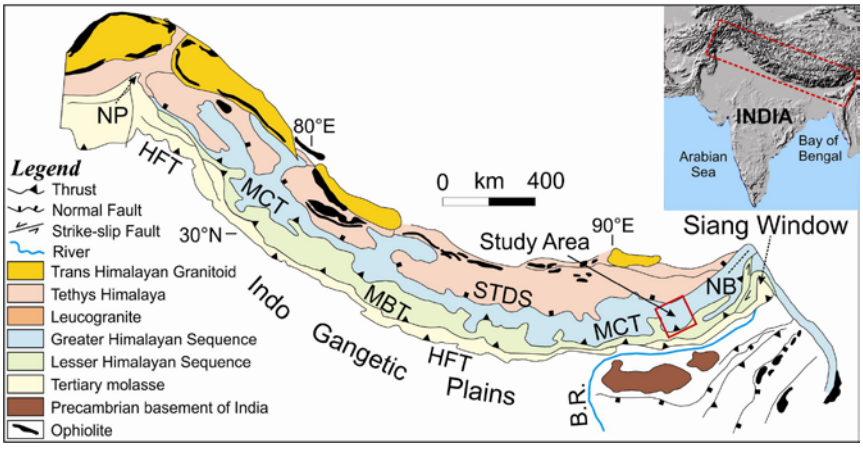

Fig. 1. *Generalized Geological map of Himalaya (after Gansser, 1974) shows study area in Eastern Himalaya. Inset: Location of Himalayan range is shown in a map of India.*
NP – Nanga Parbat,
NB – Namche Barwa,
B. R. – Brahmaputra River,
STDS – South Tibetan Detachment System,
MCT – Main Central Thrust,
MBT – Main Boundary Thrust,
HFT – Himalayan Frontal Thrust.

from the gradient of the age-elevation profile (Stüwe *et al.*, 1994; Willett and Brandon, 2002).

3. LUMINESCENCE THERMOCHRONOLOGY AND MEASUREMENTS

Herman *et al*. (2010) applied Optically Stimulated Luminescence (OSL) to estimate the temporal evolution of relief and exhumation rates within recent glacial cycles in the Southern Alps of New Zealand. The OSL thermochronometer offers a relative ease of sample preparation and analytical procedures in comparison to fission track, (U-Th)/He and Ar-Ar techniques. However, the limitations are early saturation of quartz luminescence and possible athermal fading of feldspar signal. These limit the upper age range which additionally depends on the environmental radiation dose rate (Li and Li, 2012).

Quartz OSL decay curve comprises several components, typically ultrafast, fast, medium and slow components, with variable dose saturation levels (Rhodes, 1990; Singarayer and Bailey, 2003; Jain *et al*. 2008; Madhav, 2008). Using activation energy (E_a) as 1.59 eV and frequency factor (s^{-1}) of 8×10^{12} and the Dodson (1973) equation $T_c = E_a/k \ln(\gamma\tau s)$, Herman *et al.* (2010) estimated the closure temperature of the fast component of quartz OSL signal as 30-35°C for a cooling rate of 10°C/Ma. Li and Li (2012) provided a new relation to determine the cooling age, and provided ways to obtain the cooling rate directly from a plot of luminescence age versus ambient temperature. Applicability of thermoluminescene (TL) and feldspar infra-red stimulated luminescence (IRSL) also show promise and are being developed (Jain and Ankjaergaard, 2011; Li and Li, 2012).

Both separation of quartz and its OSL analyses were carried out under subdued red light conditions. From large rock samples either cube or rectangle of 2-2.5 cm^3 size was cut after removing a cm of skin, using a water cooled diamond cutter. Then the samples were crushed in a hand mortar and grain sizes between 100-250 µm were sieved. These were treated with 1N HCl to remove carbonates followed by heavy liquid separation using sodium polytungstate of density 2.60 g/cm^3 to isolate the feldspar fraction. The samples were then etched using HF (40%; 85 minutes to remove alpha irradiated skins and residual feldspars) followed by 12N HCl (40 minutes to remove fluorides). Remaining portion was sieved for 90-150 µm size fraction and then passed through a magnetic separator to remove iron-bearing heavy minerals. The purity of quartz in respect of feldspar contamination was checked using infrared stimulated luminescence (IRSL) and if the IRSL yield exceeded the background limit, the HF treatment was repeated. In a crystalline gneissic rock, separation of quartz and feldspars grains is difficult and invariably in crushed rock fragments both minerals often co-exist. Repeated HF treatment helped to reduce feldspar proportion.

The samples were analyzed in a Risoe TL-OSL reader (TL-DA-15) with blue LEDs (~470 nm) and the detection optics comprised Hoya UV 340 and Schott BG 39 filters coupled to an EMI 9235 QA photomultiplier tube. The irradiations were carried out using a 40 mCi $^{90}Sr/^{90}Y$ beta source. Equivalent dose (D_e) measurement procedure comprised small aliquot six point double-SAR cycles (Jain and Singhvi, 2001; Roberts, 2007) which used the double SAR (Single Aliquot Regeneration) protocol (Murray and Wintle, 2000; 2003) with an additional step of IRSL stimulation before OSL, to increase the proportion of Quartz OSL. A 220°C preheat was applied before OSL measurements. Quartz grains had poor sensitivity; the decay curve comprised a small fast component and higher proportions of medium and slow components. Following Herman *et al.* (2010), the fast component was used but the data using the medium components also gave similar results. The slow component analysis was beset with larger errors on account of photon counting statistics. The growth curves were fitted to a saturating exponential (**Fig. 3**) and aliquots with recycling ratio of 1±0.1 were used.

The radioactivity of samples was measured by alpha counting and gamma spectrometry for dose computation and radioactive equilibrium was assumed. Given that the grain extracts were from a rock we used a fine grain dose rate with an alpha efficiency value of 0.07 based on the range of values for TL alpha efficiency of 0.05-0.20 for fine grain samples (Singhvi *et al.*, 2001). This is an estimate and the ages will change somewhat if the values were to be different from the assumed value of 0.07. However, the change will be small as the beta dose contributes over 60-70% of the total dose. We consider the use of fine grain dose to be more appropriate than the coarse grain dose rate used by Herman *et al*. (2010). A detailed analysis of dose rate determination of such samples will be needed for a more precise application of OSL and we refer to an early effort by Plachy (1980).

The radioactivity of sample 1 (TWNG 1) was about 5 times higher. Radioactivity of other samples varied in the region of 7±4 Gy/ka. We therefore considered this being an artifact of recent enrichment due to weathering on the surface and higher zircon content. We therefore computed the range of ages for TWNG-1 using the maximum and the minimum dose rates (in the series that comprises similar rock types) for the age calculation and as a first approximation used an average age with the errors being the spread for the present analysis. The moisture content was ignored because of the crystalline nature of rock and cosmic ray contribution was also ignored as being negligible both because the samples were deeply buried at depths few meters until the recent exhumation and the overall radioactivity of the samples was higher. The results are given in **Table 1**.

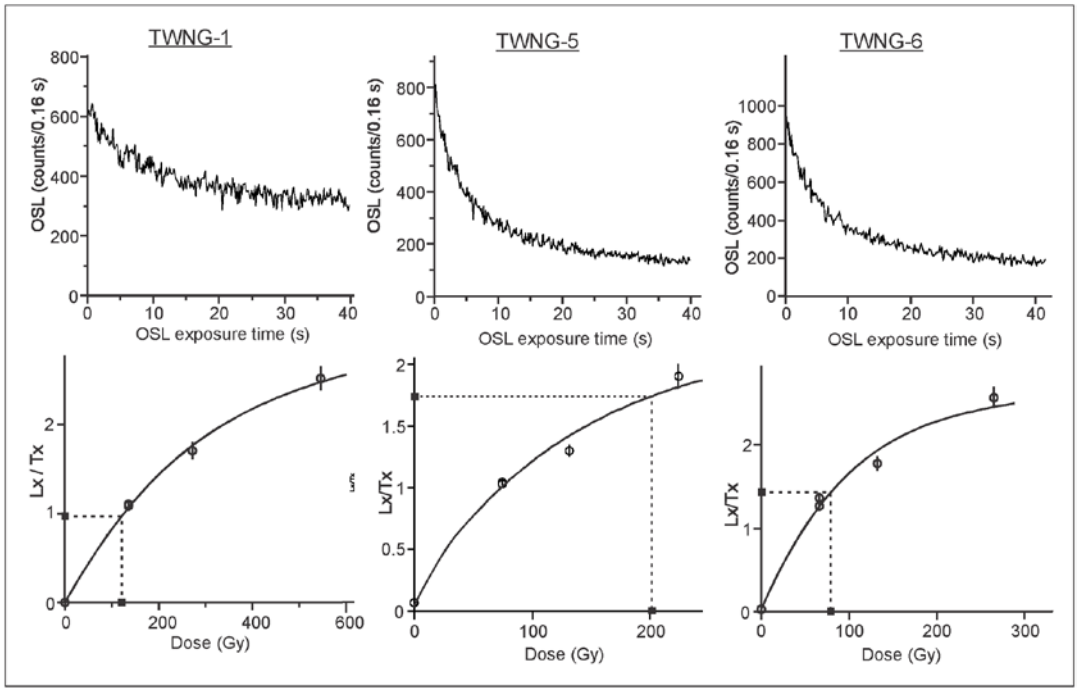

Fig. 3. *Characteristic OSL decay curves (upper row) and regenerative-dose OSL growth curves (lower row) for three samples are shown for example. Regenerative-dose points are fitted using exponential function. Natural dose is plotted on the vertical axis and corresponding equivalent dose is indicated in the horizontal axis as black filled boxes.*

Table 1. *Summary of the OSL thermochronology data.*

Sample Code	Latitude	Longitude	Altitude (m)	^{238}U (ppm)	^{232}Th (ppm)	K (%)	D_e (Gy)	1σ uncertainty (Gy)	FG Dose Rate (Gy/ka)	1σ uncertainty (Gy/ka)	Age (ka)	1σ uncertainty (ka)
TWNG-1	N 27°38'8.5"	E 91°51'31.7"	3718	22.2	192	4.54	147.6	38.5	40.4	4.1	**3.8 (23*)**	**1.0 (12*)**
TWNG-2	N 27°37'3.6"	E 91°51'47.6"	3321	3.04	16.75	2.35	183.2	20.4	6.0	0.9	**30.7**	**5.8**
TWNG-4	N 27°35'24.2"	E 91°52'47.1"	2646	1.46	9.60	1.26	53.6	3.5	3.2	0.4	**16.7**	**2.2**
TWNG-5	N 27°34'24.4"	E 91°52'25.5"	2342	3.66	18.90	4.41	203.35	33.63	8.8	0.7	**23.0**	**4.2**
TWNG-6	N 27°33'38.3"	E 91°52'43.2"	2070	5.50	25.43	4.87	133.06	6.4	10.8	0.10	**12.3**	**1.2**
TWNG-7	N 27°33'7.0"	E 91°52'47.6"	1726	3.58	15.98	3.35	70.2	9.3	7.2	0.9	**9.8**	**1.8**

Grain diameter – 200±50 μm, Layer removed – 20±5 μm, a value – 0.07, Cosmic ray contribution not taken into account; FG – Fine Grain.
**Age calculated using average dose rate of other samples*

4. INFERENCES ON DENUDATION

Of the six samples analyzed, five exhibited normal age-elevation relationship and one gave anomalous age. As alluded the topmost sample TWNG-1 had a high D_e but the computed age was low due an anomalously high dose rate. We calculated the average dose rate from other samples, and used as dose rate for sample TWNG-1. We arrived at an age of 23 ka with a spread of ±12 ka and this was generally consistent with other samples (**Table 1**). TWNG 5 gave somewhat higher age (23 ka) compared to TWNG 4 (16 ka). We consider it could be due to several factors, such as, i) only TWNG-5 exhibited the absence of an ultrafast component, suggesting some change in the luminescing mineralogy compared to others which could lead to a phase perhaps with somewhat higher closure temperature (hence higher D_e), and ii) local scale heterogeneity in radioactivity distribution, not discernible in an analysis of the bulk sample.

Least square error weighted regression of the data gave a slope of 7.6 cm/yr ($r^2 = 0.54$) as the erosion rate in a ~21 ka period from ~31 till ~10 ka. Since the slope of a line is a mathematical fit controlled dominantly by two end points and its error, we consider the slope in this estimate only as the apparent rate. The age-elevation profile assumes horizontal isotherm which lies at a constant depth. Interestingly ^{40}Ar-^{39}Ar thermochronology data show cooling ages varying from 7.2±0.7 to 4.5±0.5 Ma while AFT cooling ages on the same samples

ranged from 4.1±0.4 to 1.0±0.1 Ma (De Sarkar *et al*., 2012; Mathew *et al*., 2013). While a discussion on AFT and Ar-Ar thermochronology data measurement is dealt elsewhere (Mathew *et al*., 2013). We mention these ages to suggest that the least square error weighted regression of the data in the AFT age-elevation profile (**Fig. 4**) give distinctive slopes. This suggests that on a longer term the region had a non-uniform exhumation in the hanging wall of MCT. The data further suggest that between 7.2 to 4.5 Ma and 4.1 to 1.8 Ma the rocks exhumed at a slower rate of ~0.6 and 0.5 mm/yr respectively, however, post 1.8 Ma it experienced rapid exhumation at the rate of ~2.5 mm/yr (De Sarkar *et al.,* 2012; Mathew *et al.*, 2013) and this accentuated of 5.5 mm/yr during the past 10 ka.

The lag time between AFT and OSL ages implies cooling rates in the range of ~40 to 100°C/Myr. Li and Li (2012)'s numerical simulation models on closure temperatures for different cooling rates suggests an effective closure temperature of 39 and 42°C for cooling rates 50 and 100°C/Myr respectively. Based on these, an effective closure temperature of 40±5°C for quartz OSL was used in the study (**Fig. 4**). An effective closure temperature of 134±5°C for AFT and 370±10°C for biotite Ar-Ar were determined using the CLOSURE programme of Brandon *et al*. (1998).

In regions of high exhumation or erosion rates such as the present region in Higher Himalayan zone, thermal field of upper crust is influenced by erosion and advective heat transfer. This results in an advection-dominated thermal field that is less responsive to basal heat flow, thermophysical properties and parameters (Mancktelow and Grasemann, 1997; Stüwe *et al.*, 1994; Ehlers, 2005; Whipp *et al.*, 2007). Lateral components associated with the rock uplift and large variation in topographic wavelength do affect the exhumation path, however, errors associated with the thermochronological system accommodate such variations. This suggests that in practice for such cases of rapid exhumation, a complex 3-D modeling approach may not be required in order to arrive at a realistic estimate of exhumation rates. Young OSL ages, high rates of erosion and near vertical sampling indicate a vertical transect and therefore, make it plausible to suggest that only the vertical thermal advection and thermal conduction are needed to reconstruct exhumation/erosion history.

A one-dimensional (vertical) approach to thermal modelling (AGE2EDOT; Ehlers *et al*., 2005) was therefore used to estimate average erosion rates for the time period represented by OSL data assuming steady and constant erosion rate. In order to determine the range of erosion rates, geologically realistic values of thermal diffusivity (κ, km^2/Myr), uniform internal heat (H_T, °C/Myr), surface temperature (T_s, °C) and surface thermal gradient for no erosion (G_T, °C/km) were used to solve a steady-state thermal field equation (Reiners and Brandon, 2006). The values of κ, H_T and G_T were varied keeping the layer thickness (L) and T_s constant.

The input parameter values for κ used were 2.2 and 3.4 Wm^{-1}K^{-1} (Ray *et al.*, 2007). We used heat production values (H_T) of Whipp *et al.* (2007) in the range between 0.8 and 3.5 μWm^{-3}. As exhumation is dominated by erosional advection, the input of geothermal gradient was varied between 25 and 40°C km^{-1}. Surface temperature (T_s) was taken as 5°C. A 30 km depth (L) was used being the depth of the basal decollement of the Main Himalayan Thrust. Calculations were carried out for maximum and minimum values of thermal conductivity, geothermal gradient and heat production. We narrowed down to four solutions that cover the upper and lower limits of the thermophysical properties of rocks in the Higher Himalaya. The output of AGE2EDOT program for the above

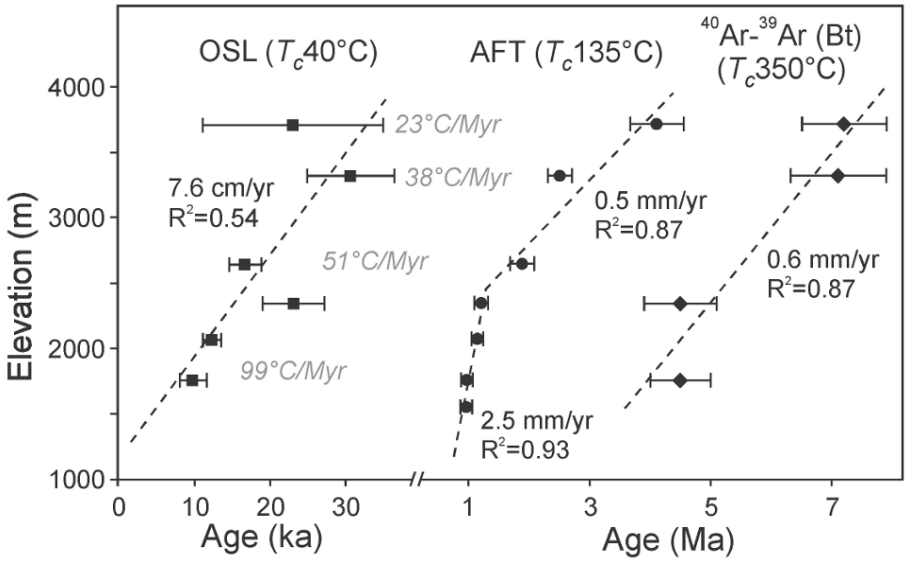

Fig. 4. *Age vs. elevation plot for OSL, AFT and Ar-Ar thermochronometric data. Effective closure temperatures (T_c) for each thermochronometric system are indicated. Cooling rates have been derived using two thermochronometer data. Cooling rates are depicted in grey italics.*

inputs is shown in **Fig. 5** that depicts the relationship between OSL age to the calculated erosion rate for the maximum and minimum values of heat production. **Table 2** shows summary of the thermal modelling result of the **Fig. 5**. Modelling data indicate that initially the erosion rate was 2.5 mm/yr during 31-16 ka and this increased gradually to 5.5 mm/yr around 10 ka (**Fig. 4**).

We consider that a steady exhumation of ~0.5 mm/yr began during Late Miocene (7.2 Ma) and continued up to 1.8 Ma when Early Pleistocene glaciation had reached its maximum. Pronounced glacial activity caused rapid erosion that carved out *U* shaped valleys. Melt water removed the glacial load and formed deep incised valleys along its path. Steep valley slopes aided landslide on valley walls causing extensive denudation. Such an accentuated erosional activity attracted mid-crustal partial melt towards the weak stress zone beneath the valley, resulting in erosion-induced tectonic uplift during >1 Ma as revealed by AFT analysis. OSL thermochronology results, however, demonstrate rapid increase in the erosional activity over ~21 ka period from ~31-10 ka. We suggest that the OSL ages document the erosional activities, rather, than exhumation since the isostatic response to erosion takes a longer time (in the range of Ma) to respond and over thousand year time scales its effects is minuscule.

The initial erosion rate of 2.5 mm/yr during Late Pleistocene progressively increased to 5.5 mm/yr during the Early Holocene. The erosion rate during Late Pleistocene was comparable to the exhumation rate (2.5 mm/yr) at ~1 Ma. OSL ages of the two middle samples (TWNG 4 and 5) incidentally coincide with the warm period of Marine Isotope Stage (MIS) 2, whereas the two bottommost samples (TWNG 6 and 7) coincide with the warm period of MIS 1. A rapid increase in erosion rate between ~16 to ~10 ka is documented. We suggest that the OSL ages, therefore, manifest the denudational activity over millennial time scales in comparison to the exhumation process revealed by the relatively higher temperature thermochronometers.

Table 2. *AGE2EDOT 1-D model derived erosion rates.*

Sample	OSL Ages (ka)	Erosion Rates Quartz OSL age (mm/a)		Average Erosion Rate (mm/a)
		Heat Production		
		0.8 μWm^{-3}	*3.0 μWm^{-3}*	
TWNG 1	35.0±5.0	2.8	1.8	2.3±0.5
TWNG 2	30.7±5.8	3.0	2.0	2.5±0.5
TWNG 4	16.7±2.2	4.8	3.2	4.0±0.8
TWNG 5	15.0±2.0	5.0	3.5	4.2±0.8
TWNG 6	12.3±1.2	6.0	4.0	5.0±1.0
TWNG 7	9.8±1.8	6.5	4.5	5.5±1.0

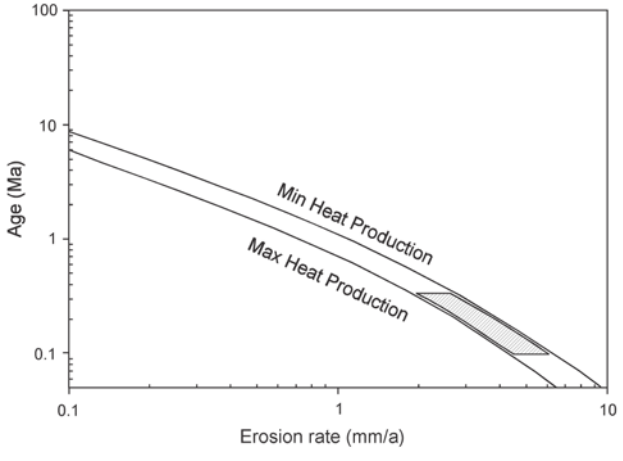

Fig. 5. *AGE2EDOT model result for OSL thermochronology data revealing increase in erosion rate with decreasing age.*

5. CONCLUSIONS

The present study used quartz OSL as a very low-temperature thermochronometer and followed initial study of Herman *et al*. (2010), that demonstrated potential of quartz luminescence as thermochronometer. In this first application of OSL thermochronology in Himalaya, we additionally used AFT and ^{40}Ar-^{39}Ar thermochronology to deduce million to thousand year time scale history of exhumation and erosion.

Use of 1-D modelling approach gave a denudation rate of 2.5 mm/yr increasing gradually to 5.5 mm/yr close to 10 ka. The initial erosion rate is comparable to the AFT exhumation rate of 2.5 mm/yr. We suggest that the extensive denudation was initiated during the Late Pleistocene and this continued into the Holocene. The OSL ages suggest that during the MIS 1 and 2, the warmer periods during the Late Pleistocene and early Holocene caused increased erosion in the Greater Himalayan rocks of western Arunachal Pradesh.

ACKNOWLEDGEMENTS

GM and KP acknowledge the funding provided by the Department of Science and Technology (DST) (IR/S4/ESF-04/2003). GM thanks IIT-Bombay for the financial support from MHRD-IRCC to attend APLED-3 workshop in Okayama, Japan. SDS thanks CSIR, HRDG for the JRF fellowship. The authors thank the Guest Editor Dr. Shin Toyoda and reviewers for the valuable constructive comments that helped to improve the MS considerably. AKS acknowledges Department of Science and Technology (DST), Govt. of India for the award of J.C. Bose National Fellowship.

REFERENCES

Brandon M, Roden-Tice M and Garver J, 1998. Late Cenozoic exhumation of the Cascadia accretionary wedge in the Olympic Mountains, north-west Washington state. *Geological Society of America Bulletin* 110(8): 985-1009, DOI 10.1130/0016-7606(1998)110<0985:LCEOTC>2.3.CO;2.

Burbank DW, 2002. Rates of erosion and their implications for exhumation. *Mineralogical Magazine* 66(1): 25-52, DOI 10.1180/0026461026610014.

De Sarkar S, Chauhan N, Mathew G, Pande K, and Singhvi AK, 2012. Late Pleistocene rapid denudation, million to thousand year scale. 3rd Asia Pacific Conference on Luminescence and Electron Spin Resonance Dating, Japan. *Advances in ESR Applications* 29: 22.

Dodson MH, 1973. Closure temperature in cooling geochronological and petrological systems. *Contribution to Mineralogy and Petrology* 40(3): 259-274, DOI 10.1007/BF00373790.

Ehlers TA, 2005. Crustal thermal processes and the interpretation of thermochronometer data, in Low-Temperature Thermochronology: Techniques, Interpretations, and Applications. In: Reiners PW and Ehlers TA, eds., *Low-Temperature Thermochronology: Techniques, Interpretations, Applications*. Reviews in Mineralogy and Geochemistry 58: 315-350, DOI 10.2138/rmg.2005.58.12.

Ehlers TA, Chaudhri T, Kumar S, Fuller CW, Willett SD, Ketcham RA, Bradon MT, Belton DX, Kohn BP, Gleadow AJW, Dunai TJ and Fu FQ, 2005. Computational tools for low-temperature thermochronometer interpretations. *Reviews in Mineralogy and Geochemistry* 58: 589-622, DOI 10.2138/rmg.2005.58.22.

Gansser A, 1974. Himalaya. In: Spenser AM, ed., Mesozoic Cenozoic Orogenic Belts: Data for Orogenic Studies. *Geological Society of London Special Publication* 4: 267-278.

Gansser A, 1983. *Geology of the Bhutan Himalaya*: Boston, Birkhauser Verlag, 181 p.

Herman F and Braun J, 2006. Fluvial response to horizontal shortening and glaciations: a study in the Southern Alps of New Zealand. *Journal of Geophysical Research* 111, F01008, DOI 10.1029/2004JF000248.

Herman F, Rhodes EJ, Braun J and Heiniger L, 2010. Uniform erosion rates and relief amplitude during glacial cycles in the Southern Alps of New Zealand, as revealed from OSL-thermochronology. *Earth Planetary Science Letters* 297(1-2): 183-189, DOI 10.1016/j.epsl.2010.06.019.

Hodges KV, 2000. Tectonics of the Himalaya and Southern Tibet from two perspectives. *Geological Society of America Bulletin* 112(3): 324-350, DOI 10.1130/0016-7606(2000)112<324:TOTHAS>2.0.CO;2.

Jain M and Ankjaergaard C, 2011. Towards a non-fading signal in feldspar: insight into charge transport and tunnelling from time-resolved optically stimulated luminescence. *Radiation Measurements* 46(3): 292-309, DOI 10.1016/j.radmeas.2010.12.004.

Jain M and Singhvi AK, 2001. Limits to depletion of green light stimulated luminescence in feldspars: implication for Quartz dating**,** *Radiation Measurements* 33(6): 883-892, DOI 10.1016/S1350-4487(01)00104-4.

Jain M, Choi JH and Thomas PJ, 2008. The ultrafast OSL component in quartz: Origin and implications. *Radiation Measurments* 43(2-6): 709-714, DOI 10.1016/j.radmeas.2008.01.005.

Li B and Li SH, 2012. Determining the cooling age using luminescence thermochronology. *Tectonophysics* 580: 242-248, DOI 10.1016/j.tecto.2012.09.023.

Mancktelow NS and Grasemann B, 1997. Time-dependent effects of heat advection and topography on cooling histories during erosion. *Tectonophysics* 270(3-4): 167-195, DOI 10.1016/S0040-1951(96)00279-X.

Madhav MK, 2008. Component Specific Luminescence of Natural Mineral and their application to the dosimetry of Natural Radiation Environment. Unpubl. Ph.D thesis, ML Sukhadia University, Udaipur, India, 129p.

Mathew G, De Sarkar S, Pande K, Jonckheere R, Ratshbacher L and Phukon P, 2013. Late Miocene - Pleistocene enhanced exhumation in the Eastern Himalaya, India (In preparation)

Murray AS and Wintle AG, 2000. Luminescence dating of quartz using an improved single-aliquot regenerative-dose protocol. *Radiation Measurements* 32(1): 57-73, DOI 10.1016/S1350-4487(99)00253-X.

Murray AS and Wintle AG, 2003. The single aliquot regenerative dose protocol: potential for improvements in reliability. *Radiation Measurements* 37(4-5): 377-381, DOI 10.1016/S1350-4487(03)00053-2.

Plachy AL, 1980. An imporved determination of the internal beta ray dose rate in granite rocks and its effect on thermoluminescence dates. Unpubl. PhD thesis, Washinton University, St. Louis, USA.331p.

Ray L, Bhattacharya A and Roy S, 2007. Thermal conductivity of higher Himalayan crystallines from Garhwal Himalaya, India. *Tectonophysics* 434(1-4): 71-79, DOI 10.1016/j.tecto.2007.02.003.

Reiners PW and Brandon Mark T, 2006. Using thermochronology to understand orogenic erosion. *Annual Review of Earth and Planetary Sciences* 34: 419-466, DOI 10.1146/annurev.earth.34.031405.125202.

Reiners PW, Ehlers TA and Zeitler PK, 2005. Past, present, and future of thermochronology. In: Reiners PW and Ehlers TA, eds., *Low-Temperature Thermochronology: Techniques, Interpretations and Applications*. Reviews in Mineralogy and Geochemistry 58: 1-18, DOI 10.2138/rmg.2005.58.1.

Rhodes EJ, 1990. Optical dating of quartz from sediments. Ph.D. thesis. Oxford.

Roberts HM, 2007. Assessing the effectiveness of the double-SAR protocol in isolating a luminescence signal dominated by quartz. *Radiation Measurements* 42(10): 1627-1636, DOI 10.1016/j.radmeas.2007.09.010.

Shuster DL, Ehlers TA, Rusmore ME and Farley KA, 2005. Rapid glacial erosion at 1.8 Ma revealed by $^{4}He/^{3}He$ thermochronometry. *Science* 310: 1668-1670, DOI 10.1126/science.1118519.

Singarayer J and Bailey RM, 2003. Further investigations of the quartz optically stimulated luminescence components using linear modulation. *Radiation Measurements* 37(4-5): 451-458, DOI 10.1016/S1350-4487(03)00062-3.

Singhvi AK, Bluszcz A, Bateman M and Someshwararao M, 2001. Luminescence dating of Loess-Paleosol sequences- Methodological Aspects and Paleoclimatic implications *Earth-Science Reviews*. 54(1-3): 193-221, DOI 10.1016/S0012-8252(01)00048-4.

Stüwe K, White L and Brown R, 1994. The influence of eroding topography on steady–state isotherms: Application to fission track analysis. *Earth and Planetary Science Letters* 124(1-4): 63-74, DOI 10.1016/0012-821X(94)00068-9.

Valla PG, Shuster DL and van der Beek PA, 2011. Significant increase in relief of the European Alps during mid-Pleistocene glaciations. *Nature Geoscience* 4(10): 688-692, DOI 10.1038/ngeo1242.

Whipp Jr. DM, Ehlers TA, Blythe AE, Huntington KW, Hodges KV and Burbank DW, 2007. Plio-Quaternary exhumation history of the central Nepalese Himalaya: 2. Thermokinematic and thermochronometer age prediction model. *Tectonics* 26(3): TC3003, DOI 10.1029/2006TC001991.

Whipple KX, 2009. The influence of climate on the tectonic evolution of mountain belts. *Nature Geoscience* 2(2): 97-105, DOI 10.1038/ngeo413.

Willett SD and Brandon MT, 2002. On steady states in mountain belts. *Geology* 30(2): 175-178, DOI 10.1130/0091-7613(2002)030<0175:OSSIMB>2.0.CO;2.

Yin A, Dubey CS, Kelty TK, Gehrels GE, Chou CY, Grove M and Lovera O, 2006. Structural evolution of the Arunachal Himalaya and implications for asymmetric development of the Himalayan orogen. *Current Science* 90(2): 195-206.